Supplementary Information

Rapid one-step scalable microwave synthesis of $Ti_3C_2T_x$ MXene

Jing Zhu, Jingyi Zhang, Ruiming Lin, Benwei Fu, Chengyi Song, Wen Shang, Peng Tao*, and Tao Deng*

State Key Laboratory of Metal Matrix Composites, School of Materials Science and Engineering, Shanghai Jiao Tong University, Shanghai, 200240, China

*Email: taopeng@sjtu.edu.cn; dengtao@sjtu.edu.cn

Experimental Section

Materials

Ti_3AlC_2 powders (99.8%, 400 mesh) were purchased from Xiyan technology (Shandong) co. LTD, China. HCl (36.0～38.0%) was ordered from Sinopharm (Shanghai) and LiF was ordered from Meryer (Shanghai). All chemical reagents were of analytical grade. Deionized (DI) water was used to prepare the corresponding reaction solution.

Synthesis of $Ti_3C_2T_x$

The $Ti_3C_2T_x$ was synthesized by one-step microwave heating of the Ti_3AlC_2 powders within the HCl/LiF aqueous solution. DI water was added to HCl (12M) to prepare a diluted 9M HCl solution, and 20 ml of the dilute HCl solution was then transferred into a Teflon vessel. After that, 1.6 g of LiF was slowly added to this solution. The mixture was magnetically stirred for 5 min until the LiF was fully dissolved. In a typical process, 1 g of Ti_3AlC_2 powder was slowly added into this solution. The mixture was then placed

within a household microwave oven under an irradiation power of 200 W. The reaction mixture was irradiated for 5 min and then was cooled down for 1 min. The whole heating/cooling process was repeated three times. The obtained products were washed with DI water by repeated centrifugation at 3500 rpm for 5 min until the pH of supernatant reached 6~7. After centrifugation, aqueous dispersion was sonicated in an ice bath for 1 h and 3 h, respectively. The resultant dispersion was centrifuged at 3500 rpm for 20 min and the supernatant was collected.

Characterization

The morphologies of Ti_3AlC_2 and $Ti_3C_2T_x$ were characterized by using the scanning electron microscope (SEM, RISE-MAGNA) and the transmission electron microscope (TEM, TALOS F200X). AFM characterization was performed on the Bruker Multimode 8 system. XPS analyses were carried out by using an AXIS Ultra DLD X-ray photoelectron spectrometer under a chamber pressure of 10^{-10} mbar. The X-ray source is generated by an Al anode (1486.7 eV). X-ray diffraction was performed on the Bruker D4 diffractometer with Ni-filtered Cu Kα radiation (λ=1.5406 Å).

Photothermal performance of $Ti_3C_2T_x$ nanosheets

The near-infrared (NIR) photothermal experiments were carried out by illuminating a glass vial (1 cm in diameter) containing 0.5 ml of $Ti_3C_2T_x$ nanosheets dispersion (0.125, 0.1, 0.05, 0.02 and 0.01 mg/ml) with 808-nm laser (Shanghai Connect Fiber Optics Company). The glass vial is placed within a thermal insulative polystyrene foam during the illumination process. The temperature evolution profiles of the irradiated aqueous dispersion were recorded by a data acquisition instrument (Agilent).

Calculation of extinction coefficient

According to the Lambert-Beer Law:

$$A(\lambda) = \alpha LC \quad (1)$$

where A is the absorbance at the wavelength λ, α is the extinction coefficient, L is optical path length (1 cm), and C is the concentration of the $Ti_3C_2T_x$ nanosheets (g/L). To obtain the extinction coefficient α of $Ti_3C_2T_x$ nanosheets in 808 nm, the dependence of A/L on C is linearly fitted and the slope of the fitted curve yields α (L · g^{-1} · cm^{-1}).

Calculation of photothermal conversion efficiency

The overall energy balance for the dispersion system can be expressed as:

$$\sum_i m_i C_{p,i} \frac{dT}{dt} = Q_{Ti_3C_2T_x} + Q_{Base} - Q_{Surr} \quad (2)$$

where m and C are the mass and heat capacity of water, T is the solution temperature, $Q_{Ti_3C_2T_x}$ is the photothermal energy input from $Ti_3C_2T_x$ nanosheets, Q_{Base} is the baseline energy input from the solvent after laser illumination, and Q_{Surr} is the heat lost from the illuminated solution to surrounding air.

The 808-nm laser induced strong localized plasmon resonance effect on the surface of $Ti_3C_2T_x$. The generated photothermal energy can be calculated by:

$$Q_{Ti_3C_2T_x} = I\left(1 - 10^{-A_{808}}\right)\eta \quad (3)$$

where I is the illumination laser power (mW), A_{808} is the absorbance of the $Ti_3C_2T_x$ nanosheets at the wavelength of 808 nm, and η is the photothermal conversion efficiency.

Water can also absorb NIR light and convert it into heat. The heat gain by water during the NIR illumination (Q_{Base}) can be estimated by:

$$Q_{Base} = mC(T - T_{surr}) \quad (4)$$

where m is the mass of the water solvent (0.5 g), C is its heat capacity (4.2 J/g), T is the solution temperature, and T_{Surr} is the surrounding temperature.

In the meanwhile, the illuminated solution loses part of heat mainly through convection to the surrounding air. The heat loss (Q_{Surr}) can be calculated by:

$$Q_{Surr} = hS\left(T - T_{Surr}\right) \quad (5)$$

where h is heat transfer coefficient, S is the surface area of the vial.

Under a fixed laser illumination power, the system temperature will rise to a maximum value (T_{Max}) when the heat input $\left(Q_{Ti_3C_2T_x} + Q_{\mathrm{Base}}\right)$ is equal to the heat output (Q_{Surr}).

$$Q_{Ti_3C_2T_x} + Q_{Base} = Q_{Surr-Max} = hS(T_{Max} - T_{Surr}) \quad (6)$$

By rearranging Equation (3) and Equation (6), the laser photothermal conversion efficiency (η) of $Ti_3C_2T_x$ at 808 nm can be obtained:

$$\eta = \frac{hS(T_{\mathrm{Max}} - T_{\mathrm{Surr}}) - Q_{\mathrm{Base}}}{I\left(1 - 10^{-A_{808}}\right)} \quad (7)$$

By independently using a sample containing pure water (0.5 ml), Q_{Base} was measured to be 1.1512 mW. The T_{Surr} and T_{Max}were measured to be 17 °C and 69.8°C, respectively. In addition, the absorbance of $Ti_3C_2T_x$ nanosheets at 808 nm is 1.2113, I is 735 mW.

To get the hS, a dimensionless constant θ was used:

$$\theta = \frac{T - T_{\mathrm{Surr}}}{T_{\mathrm{Max}} - T_{\mathrm{Surr}}} \quad (8)$$

and a sample system time constant τ_S was defined as:

$$\tau_S = \frac{\sum_i m_i C_{p,i}}{hS} \quad (9)$$

By substituting (8) and (9) into Equation (2), the following equation can be obtained:

$$\frac{d\theta}{dt} = \frac{1}{\tau_S}\left[\frac{Q_{Ti_3C_2T_x} + Q_{Base}}{hS(T_{Max} - T_{\mathrm{Surr}})} - \theta\right] \quad (10)$$

When the laser was shut off, the heat input $(Q_{Ti_3C_2T_x} + Q_{Base})$ was zero and the system cooled down, the following dependence can be obtained:

$$dt = -\tau_s \frac{d\theta}{\theta} \quad (11)$$

Integrating Equation (11) yields the following expression:

$$t = -\tau_s ln(\theta) \quad (12)$$

Figure S6a depicts the temperature evolution profile when the $Ti_3C_2T_x$ dispersion

was illuminated by the 808-nm laser (1.5 W/cm^2) for 480 s followed by natural cooling. By linearly fitting the dependence of t versus $-ln(\theta)$ at the cooling stage, the slope of the fitted curve (Figure S6b) yields τ_s (331). According to Equation (9), the hS was calculated to be 6.35 mW/°C. By substituting this value of hS into Equation (7), the photothermal conversion efficiency (η) of $Ti_3C_2T_x$ nanosheets at 808 nm was calculated to be 48.7%.

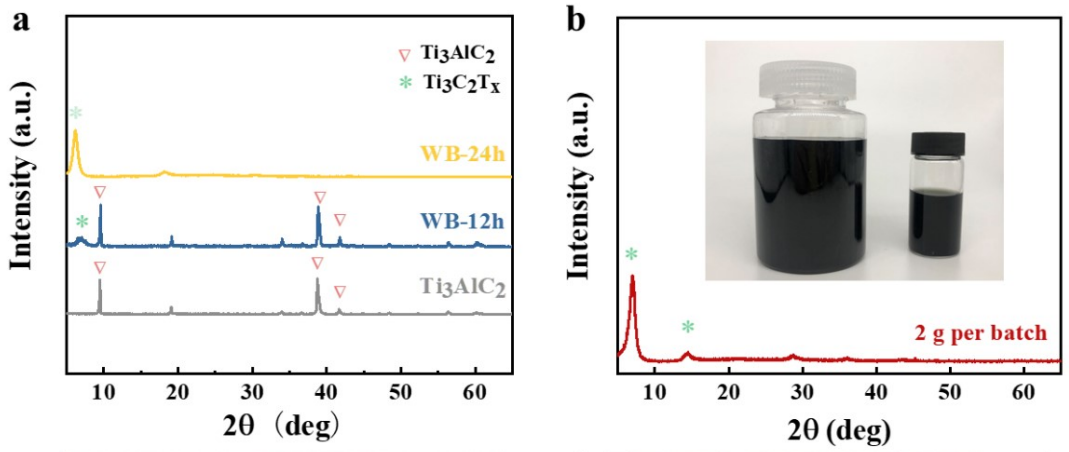

Fig. S1 (a) XRD patterns of Ti_3AlC_2 and the products etched for 12 h, 24 h by the typical water bath synthetic method. (b) XRD pattern of $Ti_3C_2T_x$ when the microwave synthesis is scaled to 2 g per batch. The inset images show stable aqueous dispersion of the obtained $Ti_3C_2T_x$ (0.1 g and 2 g per batch).

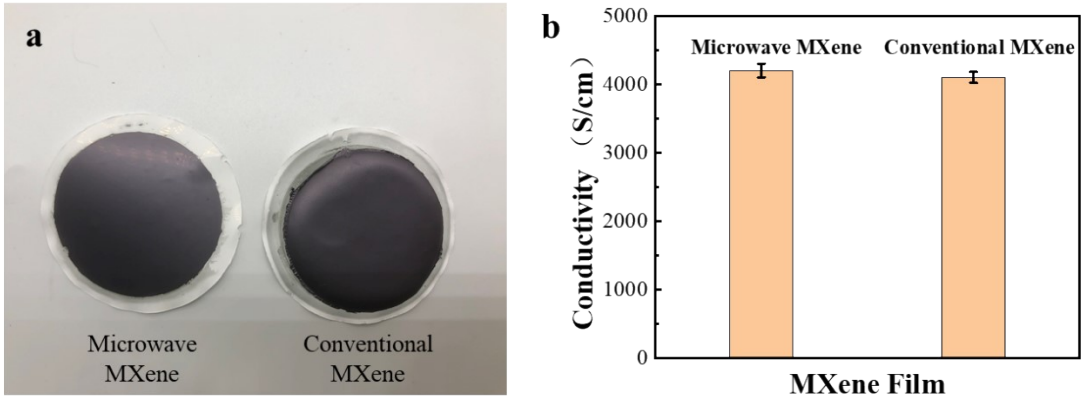

Fig. S2 (a) Photograph of MXene films prepared through vacuum filtration and drying. (b) Comparison of electrical conductivity of microwave-synthesized and conventional heating-synthesized MXene films.

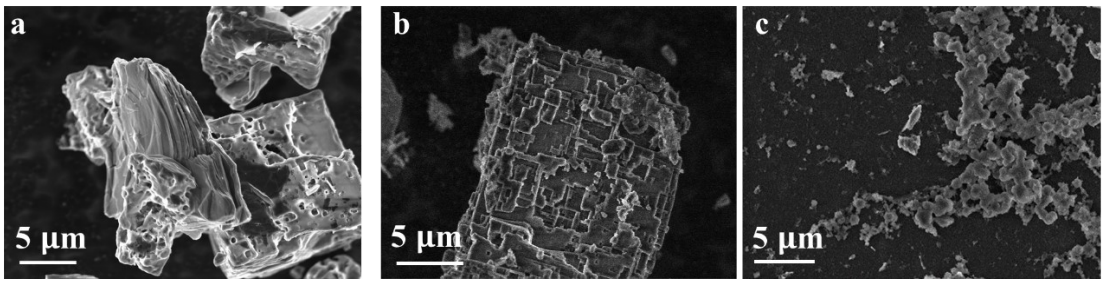

Fig. S3 SEM images of etched products when the microwave power is (a) 400 W, (b) 600 W and (c) 800 W.

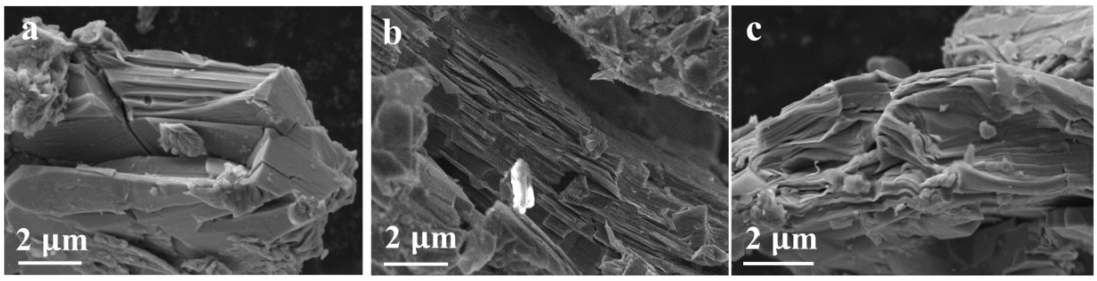

Fig. S4 SEM images of the etched products when the concentration of HCl is (a) 6 M, (b) 9 M, (c) 12 M.

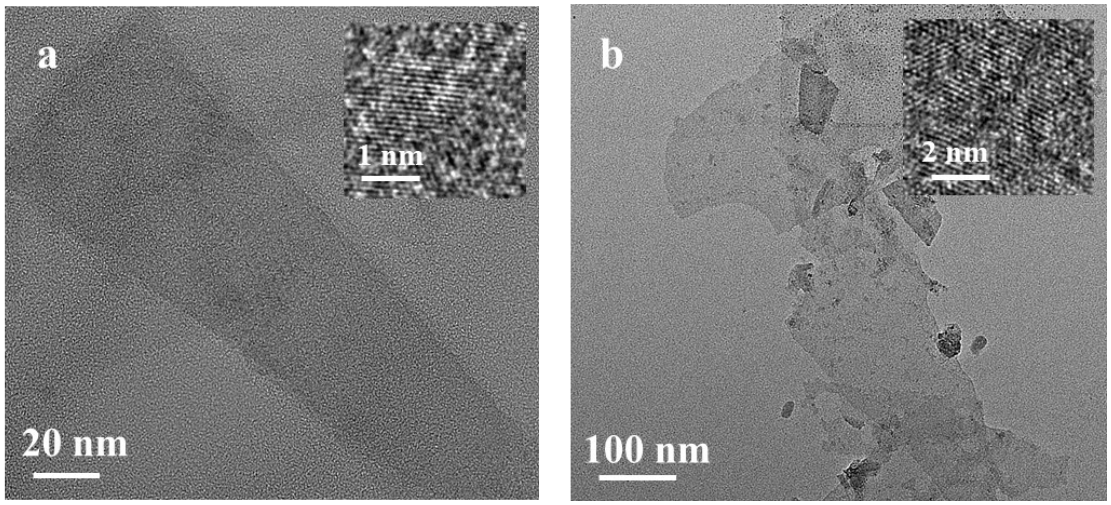

Fig. S5 (a, b) TEM images of $Ti_3C_2T_x$ prepared by the microwave heating method. The inset is the corresponding HR-TEM image.

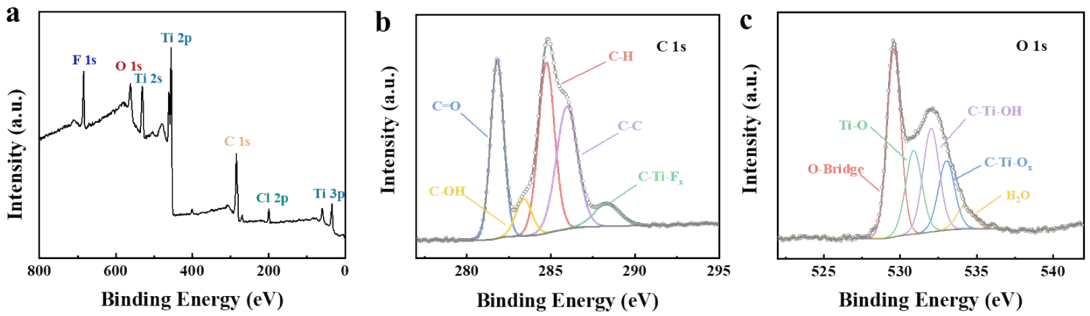

Fig. S6 (a) XPS survey spectrum of $Ti_3C_2T_x$ powders. High resolution XPS spectra of (b) C 1s and (c) O 1s.

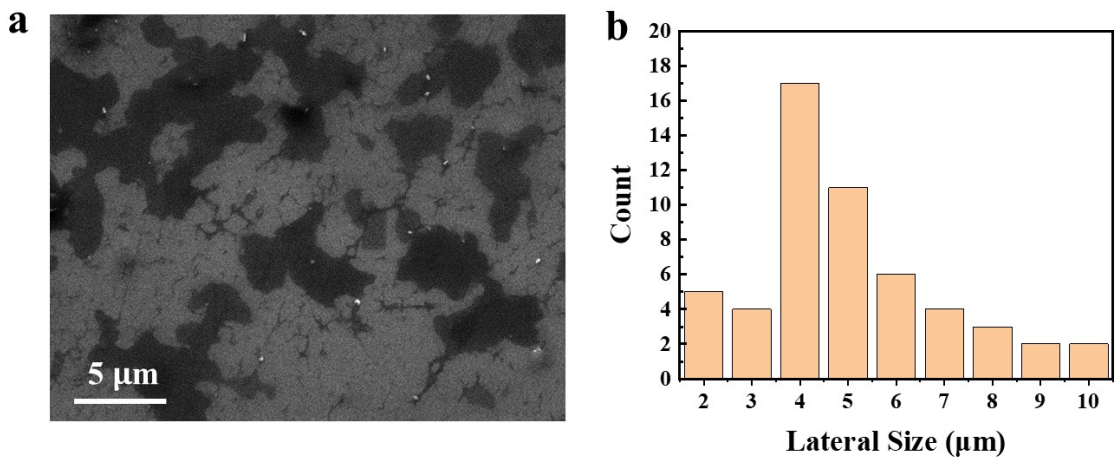

Fig. S7 (a) SEM image of $Ti_3C_2T_x$ sheets after sonicating the etched products for 1 h. (b) Lateral size distribution of the $Ti_3C_2T_x$ sheets after sonication for 1 h.

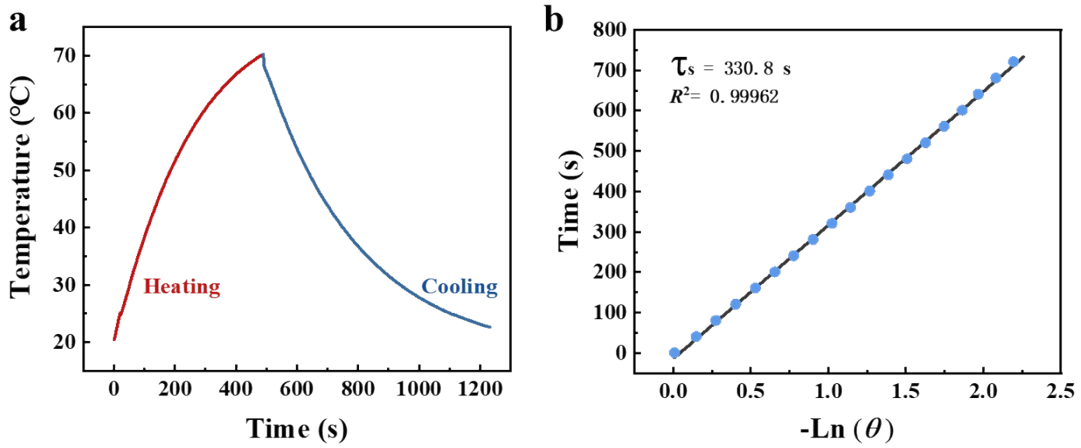

Fig. S8 (a) Temperature profile of aqueous dispersion of $Ti_3C_2T_x$ nanosheets (0.02 mg/ml) under illumination of a NIR laser (808 nm, 1.5 W/cm^2). The laser was turned on for 480 s, and then the laser was turned off for natural cooling. (b) Linear fitting *t* with -Ln(θ) during natural cooling.

Table. S1 XPS peak fitting results of Ti 2p, C1s and O1s for microwave-synthesized $Ti_3C_2T_x$

Region	Position	FWHM	%content	Assigned to
Ti 2p 3/2	455.31	1.75	53.59	Ti-C
	456.91	1.58	25.86	Ti(ii)
	458.59	1.58	14.85	Ti(iii)
	460.84	1.58	5.70	TiO_2
C 1s	281.81	0.9	26.25	C-Ti
	283.39	1.13	6.76	C-Ti-O
	284.74	1.13	31.24	C-C
	285.95	1.47	29.16	C-O
	288.33	1.8	6.58	C=O
O 1s	529.59	1.04	35.97	O-Bridge
	530.88	1.25	19.14	C-Ti-O_x
	532.02	1.25	23.77	Ti-O
	533.02	1.25	15.84	C-Ti-OH
	534.22	1.25	5.28	TiO_2